Self-ignition Combustion Synthesis of $TiFe_{1-X}Mn_X$ Hydrogen Storage Alloy

NaotoYasuda, Ryuta Wakabayashi, Sino Sasaki, Noriyuki Okinaka,

Tomohiro Akiyama*

Center for Advanced Research of Energy Conversion Materials, Hokkaido University, Kita 13 Nishi 8, Kita-ku, Sapporo, Hokkaido 060-8628, Japan

Phone: +81-11-706-6842

Fax: +81-11-726-0731

*Corresponding Author: takiyama@eng.hokudai.ac.jp

Abstract (147 words)

The paper describes the *self-ignition combustion synthesis (SICS)* of the hydrogen storage alloy $TiFe_{1-X}Mn_X$ (X = 0, 0.1, 0.2, 0.3, and 0.5) in a hydrogen atmosphere, where the hydrogenation properties of the products are mainly examined. In the experiments, the well-mixed powders of Ti, Fe, and Mn in the molar ratio of 1:1−X:X were uniformly heated up to 1473 K, and then were cooled naturally in pressurized hydrogen at 0.9 MPa. All products were successfully synthesized by utilizing the exothermic reaction, which occurred at around 1358 K. The XRD analysis showed that SICS generated $TiFe_{1-X}Mn_X$ in the range of X value from 0 to 0.3. All SICSed products absorbed hydrogen smoothly at 298 K at an initial pressure of 4.1 MPa. Most significantly, $TiFe_{0.8}Mn_{0.2}$ improved the dual plateau property. The results revealed that SICS was quite effective for producing the hydrogen storage alloy $TiFe_{1-X}Mn_X$.

Introduction

It is well known that titanium iron (TiFe), a typical AB type hydrogen storage alloy, has many advantages such as high cost performance and abundance in resources, moderate conditions for hydrogenation and dehydrogenation and relatively large hydrogen storage capacity of 1.8 mass% [1]. However, TiFe has not been used for practical purposes, mainly because it requires a quite tough activation treatment. Further, it requires a cyclic procedure of heating up to 673 K at vacuum, cooling down to room temperature, and pressurizing hydrogen up to 4 MPa. This procedure must be repeated over ten times. Even worse, TiFe has dual plateaus in the PCT diagram, where the equilibrium pressure of β-hydride is different from that of γ-hydride. For this reason, the difference in pressure for hydrogenating and dehydrogenating is relatively large [2−5].

Recently, the activation behavior of TiFe was improved significantly by an innovative manufacturing process. In 1997, the use of hydriding combustion synthesis (HCS) that was based on the *self-propagation mode* was proposed [6, 7]. Since then, it has been extensively used for improving the activation behavior. One example is the direct production of the metal hydride of a Mg-based alloy [8]. HCS has many advantages such as shortening the processing time, purifying the product, boosting energy efficiency, and hydriding an alloy directly. Saita et al. [9] reported that HCS

using excess Ti powder activates TiFe more easily when compared to the conventional melting method. The products exhibited good cycling property; however, this method was not suitable for the mass production of TiFe because the excess Ti was needed as the heat source. In contrast, the *self-ignition mode* of combustion synthesis is better than the self-propagation mode, where the mixed powders of the desired compositions are uniformly heated up to the ignition point without using excess Ti. In this study, we call this method *self-ignition combustion synthesi*s (*SICS*). Very recently, Wakabayashi et al. [10, 11] reported that TiFe based alloys were successfully produced by SICS.

To solve the two problems in hydrogenation properties of TiFe, i.e., the activation difficulty and dual plateau property, several papers reported the effect of using a third element to substitute Fe or Ti partially [12, 13]. According to reference [14−16], Mn is the most effective element used for the improvement of dual plateau property without the decrease in the hydrogen storage capacity. At the same time, Mn is also expected to improve the activation behavior of the product. All products reported were prepared by the conventional melting method, which is really time- and energy-consuming. In fact, SICS is quite attractive for producing TiFe-based alloys as mentioned above. However, no paper has been published on this matter according to a major database.

Therefore, the purpose of this study is to synthesize hydrogen storage alloys of

$TiFe_{1-X}Mn_X$ (X = 0, 0.1, 0.2, 0.3, and 0.5) by SICS in a hydrogen atmosphere for improving their activation behavior and dual plateau property, where the hydrogenation properties of the products were also investigated. TiFe-based hydrides cannot be used for hydrogen transportation; however, they will be suitable for stationary hydrogen storage system.

Experiment

The detailed explanations on the equipment and experimental procedure have been already published in the reference [10, 11], therefore only the framework of them was described here.

Fig. 1 shows the schematic diagram of the experimental apparatus. The device can be used to uniformly heat the sample up to 1773 K under a high hydrogen pressure of up to 1.0 MPa. The reactor has two R-type thermocouples that were used for the control and measurement of temperatures inside the reactor. The pressure inside the reactor can be controlled using the On–Off controller.

Table 1 Mixing ratio of reagents for producing each sample.

X value ($TiFe_{1-X}Mn_X$)	Sample name	Molar ratio		
		Ti	Fe	Mn
0	TF	1	1	-
0.1	TFM10	1	0.9	0.1
0.2	TFM20	1	0.8	0.2
0.3	TFM30	1	0.7	0.3
0.5	TFM50	1	0.5	0.5

Table 1 shows the defined sample name and the mixing ratio of samples used in SICS.

First, 200 g of these reagents (Kojundo Chemical Laboratory Co., Ltd.), Ti (99.9%, 45 μm pass), Fe (99.9%, 3~5 μm), and Mn (99.9%, ca. 10 μm), was mixed with liquid acetone in a mixer for 30 min at room temperature in the predetermined molar

ratio shown in Table 1. The smallest reagents commercially available were selected as raw materials for maximizing contact area among raw materials. Then, each mixture was kept in a desiccator in air at 353 K for 20 h. Next, each sample was placed in a carbon crucible. An R-type thermocouple placed inside a protective alumina tube was introduced into the center of the sample. 99.99999% pure hydrogen was charged to 0.9 MPa for combustion synthesis in the self-ignition mode after repeating four times each the vacuuming process and the charging process with 99.999% pure argon in order to achieve substitution. Then, each sample was uniformly heated to 1573 K using the graphite heater. The heating rate was 1200 K/h. The preliminary test showed that the most important experimental parameter is to heat the sample temperature up to the eutectic point of Fe-Ti, 1358 K, not to keep uniform temperature distribution within the sample. Changes in the sample temperature were carefully observed. When the inside of the reactor reached a temperature of 1573 K, the heating of the sample was stopped immediately. Then, each sample was naturally cooled in the same hydrogen atmosphere.

After the experiments, each product obtained was polished so as to remove the carbon sheet from its surface and then was crushed using tungsten mortar for various evaluations. The generated phase of products was identified by X-ray diffraction (XRD) and energy dispersive X-ray spectrometer (EDS). The form of the products was

observed by a scanning electron microscope (SEM). The products, which were crushed to a diameter of 0.5~1.0 mm, were immediately placed into a stainless steel reactor for the characterization of hydrogenation behavior, and it was measured by employing a PCT measuring system (Suzuki Shokan Co., Ltd.). During the measurement of initial hydrogenation kinetics, the reactor filled with products was first evacuated for at least 1 h at room temperature, and then hydrogen with a pressure of 4.1 MPa was introduced into the reactor at 298 K. Prior to the pressure-composition-isotherm (PCT) measurement, samples were made to hydride/dehydride for around four cycles. The PCT curves were determined by Sieverts' method.

Results and Discussion

Fig. 2 shows the changes in the temperature at the center of the sample and the hydrogen pressure in the chamber during the SICS experiments of TFM20. At around 800 K, the first peak due to the exothermic reaction was observed, and then the sample temperature increased rapidly to 1050 K (step 1). It is to be noted that the corresponding hydrogen pressure decreased instantly due to the hydrogen storage reaction. Immediately after the exothermic reaction, the sample temperature decreased (step 2) and the hydrogen pressure increased. These couple reactions, step 1 and step 2, were attributed to the hydrogenation/dehydrogenation reaction of titanium, $Ti + H_2 = TiH_2 +$ 144 kJ. The generated titanium hydride must be decomposed again to titanium and hydrogen thermodynamically at temperatures exceeding around 1200 K. Therefore, it is estimated that the temperature of the sample partially reached at around 1200 K. After the endothermic reaction, the rate of the sample temperature rise decreased when compared to the heating rate of the furnace (1200 K/h). The inflection point was observed at around 1050 K, and then the rate of the sample temperature rise gradually increased. The second peak was observed at around 1358 K, which was the eutectic temperature of TiFe. Immediately, the sample temperature jumped to around 1400 K (step 3), which was attributed to the evolution of heat due to the TiFe reaction, Ti + Fe =

TiFe + 40 kJ. The result agrees with the some previous report that a combustion synthesis occurs near the eutectic temperature [17]. It is estimated that substitution products; $TiFe_{1-X}Mn_X$ alloys were generated using the reaction heat of TiFe. After the inside of the reactor reached a temperature of 1573 K, each sample was naturally cooled in the same hydrogen atmosphere. There was no unreacted titanium because the increase in the sample temperature due to the hydrogenation reaction of titanium was not observed at the cooling process. The temperature history of the other samples, TF, TFM10, TFM30, and TFM50, denoted the same tendency of TFM20. However, the intensity of the second peak decreased as the amount of Mn was increased, and the peak disappeared when the X value was 0.5 (TFM50). The decrease in the second peak was attributed to the shortage in the amount of iron that contributes to the TiFe reaction.

Fig. 3 shows the XRD patterns of the SICSed products and the raw materials of TFM50, respectively. No peaks that indicated the presence of impurities or unreacted raw materials in all products were observed. All peaks had been indexed to $TiFeH_{0.06}$, which showed that the product had extremely high purity, except in the case of TFM50. Fig. 4 shows the enlarged view of the peaks of TF, TFM10, TFM20, and TFM30, at around 79º. The peak position and intensity of TF and TFM10 were almost the same. However, the peak position and intensity of TFM20 and TFM30 shifted to smaller

diffraction angles and decreased intensity as the substituted amount increased. These results were attributed to the change in the lattice constant and the distortion of the crystal structure due to the substitution of the third element. This fact implied that Mn was partially substituted at an Fe site of the TiFe phase which had a CsCl-type structure. Accordingly, the result of the XRD analysis revealed that $TiFe_{1-X}Mn_X$ was generated by SICS.

Meanwhile, no peaks corresponding to the TiFe phase were observed in SICSed TFM50. It was difficult to identify the phase due to the low intensity. Consequently, TFM50 was synthesized using the melting method in an argon atmosphere for comparison. The detected peaks corresponded to the C14 laves phase. It had been reported that some alloys that had the laves structure formed an amorphous phase by hydrogen absorption [18]. Therefore, these results indicated that TFM50 formed the C14 laves phase structure because of excess Mn and became an amorphous phase due to hydrogen absorption.

Fig. 5 shows the SEM images of the SICSed products and the raw materials of TFM50. The products of TF and TFM10 were porous solid because the ignition of combustion synthesis took place momentarily at a temperature lower than the melting point of TiFe. The ignition was caused by the generation of the partial liquid phase at

the eutectic point of the Ti-Fe system, and this accelerated the TiFe reaction drastically. Therefore, although the product became TiFe, it did not melt completely and was porous. Since the obtained products were considerably porous, they could be easily pulverized and could have a sufficiently high reaction rate.

On the other hand, there were numerous grains whose diameter was 3-5 μm on the surface of the product of TFM50. These grains were identified as unreacted Ti by EDS analysis. This fact indicated that Ti did not completely react with Fe and Mn because the heat of the TiFe reaction decreased as the amount of Mn increased. However, the peaks corresponding to Ti were not observed by XRD analysis. Therefore, it is estimated that unreacted Ti grains were present only near the surface of the product. Moreover, there were many cracks on the surface of the product of TFM50. It indicated that the sample absorbed hydrogen during SICS because the appearance of cracks was attributed to volume expansion due to hydrogen absorption.

Fig. 6 shows the initial hydriding curves of the SICSed products with particle size in the range of 0.5-1.0 mm at 298 K and under an initial hydrogen pressure of 4.1 MPa. It should be noted that pure TF non-doped Mn absorbed hydrogen without so-called activation treatment at high temperature (673 K). It was confirmed that the SICS process contributed to improve the activation behavior of the sample since TiFe

produced by melting method does not absorb hydrogen without the activation treatment under the experimental conditions of 298 K and an initial pressure of 4.1 MPa.

Moreover, Mn substitution drastically improved the activation behavior of the product. The degree of improvement increased in proportion to the amount of substituted Mn. This result is explained by the following reasons. The density of defects such as dislocation in the TiFe phase and the surface oxide film increased due to Mn substitution. Therefore, the activation was facilitated drastically due to the increase in the permeability of hydrogen into TiFe. TFM20 stored hydrogen as much as 1.65 mass% in 60 ks. Although TF and TFM10 stored as much as around 1.4 mass% under these experimental conditions, the amount of stored hydrogen will increase at higher pressure due to PCT curves, which shall be found below.

Fig. 7 shows the PCT curves of the products that were synthesized by SICS at 298 K. The PCT curves were measured after they were fully activated at room temperature. The plateau pressure shifted to a low-pressure region and the plateau gradient increased in proportion to the amount of substituted Mn. These results were attributed to the change in the lattice constant. The thermodynamic stability of hydride increased in proportion to the lattice constant. Therefore, hydrogen atom remained at a low pressure in the lattice of the alloy when compared to TiFe alloy. In addition, since the crystal

structure of TiFe was distorted due to Mn substitution, the crystal lattice became nonuniform. Therefore, the plateau gradually slanted in proportion to the amount of Mn. It should be noted that TFM20 and TFM30 drastically improved their dual plateau properties that characterize TiFe. There were no plateaus on the PCT curves of TFM50. This result agree with the hydrogenate characteristic of an amorphous alloy [19, 20]. Moreover, it is estimated that the sample had been absorbed during naturally cooling.

Fig. 8 shows van't Hoff plots for SICSed $TiFe_{1-X}Mn_X$ (X=0 - 0.3)-H system at 0.6 mass% stored hydrogen. The plateau pressure of the products denoted the same tendency of the PCT curves at 298 K; plateau pressure and hysteresis decreased in proportion to the amount of substituted Mn. Reaction heat ΔH, hysteresis factor HF, and plateau flatness PF were calculated using the graphs in Figs. 7 and 8. Table 2 shows these properties of the $TiFe_{1-X}Mn_X$ alloy obtained by SICS. The reaction heat ΔH was calculated from the following equation: $\ln P = \Delta H/(RT) - \Delta S/R$. The value of ΔH of the product obtained by SICS increased after Mn substitution and are close to previously reported values [14]. The HF, $\ln P_a/P_d$ (P_a is absorption pressure and P_d is desorption pressure), which was obtained with an H/M ratio of 0.3 at 298 K from the PCT curves, decreased in proportion to the amount of Mn substituted; its value was 0.73–1.15. An H/M ratio of 0.3 is equivalent to approximately 0.6 mass%. The PF, d(ln Pd)/d(H/M),

which was obtained from the PCT curve at 298 K, increased in proportion to the amount of Mn substituted; its value was 0.20–3.03.

Table 2 Additional properties of $TiFe_{1-X}Mn_X$ alloys obtained by SICS.

Sample name	Reaction Heat ΔH[a] (kJ/mol-H_2)	Hysteresis Factor HF[b] (ln Pa/Pd)[c]	Plateau Flatness PF[d] d(ln Pd)/d(H/M)
TF	-22.4	1.15	0.20
TFM10	-23.9	1.04	0.97
TFM20	-28.4	0.78	1.72
TFM30	-29.3	0.73	3.03

[a] These data for hydride formation were calculated from the plot of Fig. 8 and the following relationship; $\ln P = \Delta H/(RT) - \Delta S/R$.

[b] These data were obtained using a hydrogen-to-metal ratio (H/M) of 0.3 at 298K.

[c] P_a and P_d are absorption and desorption plateau pressures.

[d] These data refer to the principal plateau at 298 K.

Conclusions

The *self-ignition combustion synthesis* (SICS) of hydrogen storage alloy $TiFe_{1-X}Mn_X$ (X = 0, 0.1, 0.2, 0.3, and 0.5) in a hydrogen atmosphere was experimentally studied and the following conclusions were derived.

1) SICS synthesized $TiFe_{1-x}Mn_x$ hydrogen storage alloys successfully in a hydrogen atmosphere.

2) All SICSed products, including pure TiFe without Mn doping, absorbed hydrogen at 298 K smoothly at an initial pressure of 4.1 MPa. In addition, the substitution of Mn drastically improved the activation behavior of the product.

3) The alloy of $TiFe_{0.8}Mn_{0.2}$ (TFM20) significantly improved the dual plateau properties of original TiFe to a flat plateau. The value of 1.65 mass% in hydrogen storage capacity of TFM20 was the largest among all products.

The results also demonstrate that SICS is quite a useful process for producing $TiFe_{1-x}Mn_x$ hydrogen storage alloy from the easy control of desired compositions and uniform compositions without gravity segregation.

References

[1] Reilly JJ, Wiswall Jr RH. Formation and properties of iron titanium hydride. Inorg Chem 1974;13(1):218–22.

[2] Wenzl H. FeTi and lithium hydrides: properties and applications for hydrogen generation and storage. J Less-Common Met 1980;74:351–61.

[3] Sandrock GD, Goodell PD. Surface poisoning of $LaNi_5$, FeTi and (Fe, Mn)Ti by O_2, CO and H_2O. J Less-Common Met 1980;73:161–8.

[4] Schlapbach L, Seiler A, Stucki F. Surface segregation in iron-titanium (FeTi) and its catalytic effect on hydrogenation. II: AES and XPS studies. Mat Res Bull 1978;13:1031-7.

[5] Schober T. On the activation of iron-titanium for hydrogen storage. J Less-Common Met 1983;89:63–70.

[6] Dolukhanyan SK, Hakobyan HG, Aleksanyan, AG. Combustion of metals in hydrogen and hydride production by self-propagating high-temperature synthesis. Int J Self-Propagating High-Temp Synthesis 1992;1:530-535.

[7] Akiyama T, Isogai H, Yagi J. Hydriding combustion synthesis for the production of hydrogen storage alloy. J Alloys Compd 1997;252:1–4.

[8] Saita I, Li L, Saito K, Akiyama T. Pressure–composition–temperature properties of

hydriding combustion synthesized Mg2NiH4. Mater Trans 2002;43:1100–4.

[9] Saita I, Sato M, Uesugi H, Akiyama T. Hydriding combustion synthesis of TiFe. J Alloys Compd 2007;446–447:195–9.

[10] Wakabayashi R, Sasaki S, Saita I, Sato M, Uesugi H, Akiyama T. Self-ignition combustion synthesis of TiFe in hydrogen atmosphere. J Alloys Compd 2009;480:592–5

[11] Wakabayashi R, Sasaki S, Akiyama T. Self-ignition combustion synthesis of oxygen-doped TiFe. Int J Hydrogen Energy 2009; in press

[12] Mintz MH, Vaknin S, Biderman S, Hadari Z. Hydrides of ternary $TiFe_xM_{1-x}$ (M = Cr, Mn, Co, Ni) intermetallics. J Appl Phys 1981;52:463–7.

[13] Lee S-M, Perng T-P. Correlation of substitutional solid solution with hydrogenation properties of $TiFe_{1-x}M_x$ (M = Ni, Co, Al) alloys. J Alloys Compd 1999;291:254–61.

[14] Schober T, Dieker C. The system FeTi-H and $Fe_{0.85}Mn_{0.15}Ti$-H: hydrides, phase relationships and activation. J Less-Common Met 1984;104:191–7.

[15] Miller HI, Murray J, Laury E, Reinhardt J, Goudy SJ. The hydriding and dehydriding kinetics of FeTi and $Fe_{0.9}TiMn_{0.1}$. J Alloys Compd 1995;231:670-674

[16] Lanyin S, Fangjie L, Deyon B. An advanced TiFe series hydrogen storage material with high hydrogen capacity and easily activated properties. Int J Hydrogen Energy 1990;15:259–262.

[17] Kohno H, Akiyama T, Kobayashi T, Yagi J. Morphology of combustion-synthesized Mg_2Ni. J Japan Inst Metals 1997;61:166–70.

[18] Aoki K, Masumoto T. Amorphization of intermetallic compounds by hydrogen absorption. Nippon Kinzoku Gakkai Kaiho 1989;28:803-9.

[19] Aoki K, Masumoto T. Hydrogen absorption characteristics of amorphous alloys. Nippon Kinzoku Gakkai Kaiho 1984;23(10):818-25.

[20] Aoki K, Kamachi M, Masumoto T, Thermodynamics of hydrogen absorption in amorphous zirconium-nickel alloys. J Non-cryst Solids 1984;62:679-84.

Acknowledgements

This research was partly supported by the Ministry of the Environment, Japan, under the project “Development of Hydrogen Freezer Using Industrial Waste Heat or Solar Heat for Reducing CO2 Emission.”

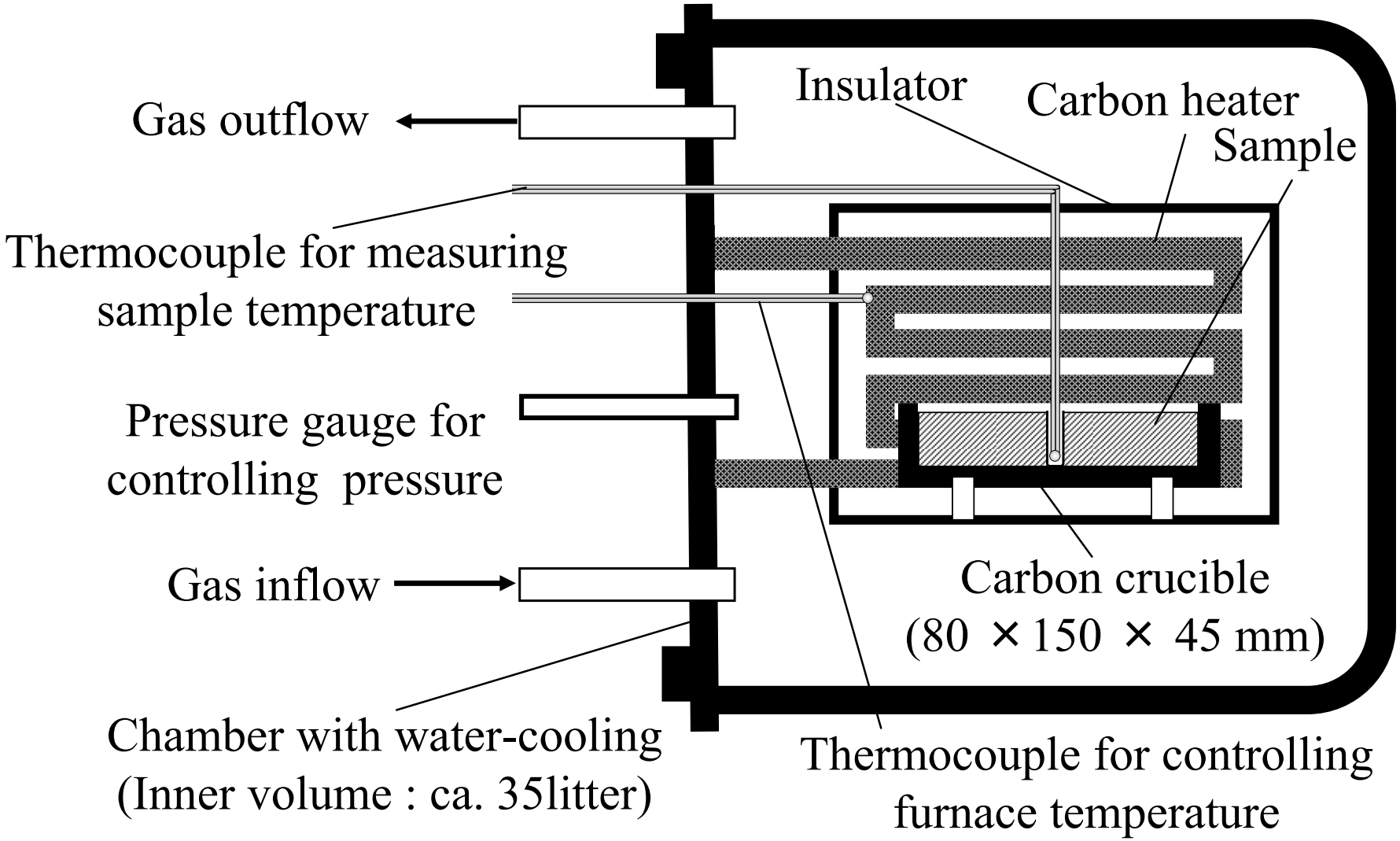

Fig. 1 Schematic diagram of *Self-ignition combustion synthesis* (SICS) reactor

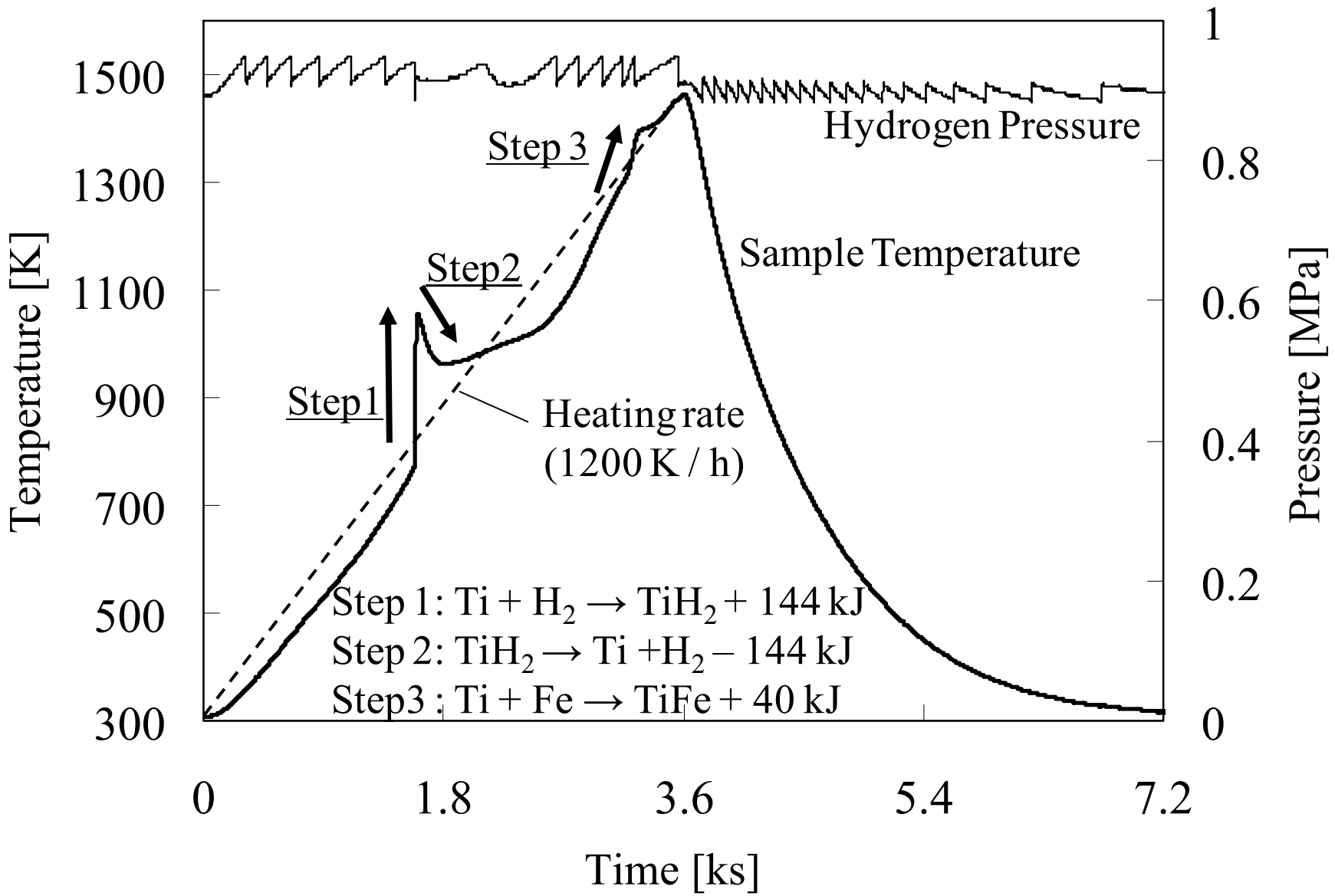

Fig. 2 Changes in sample temperature and hydrogen pressure during SICS experiment of TFM20.

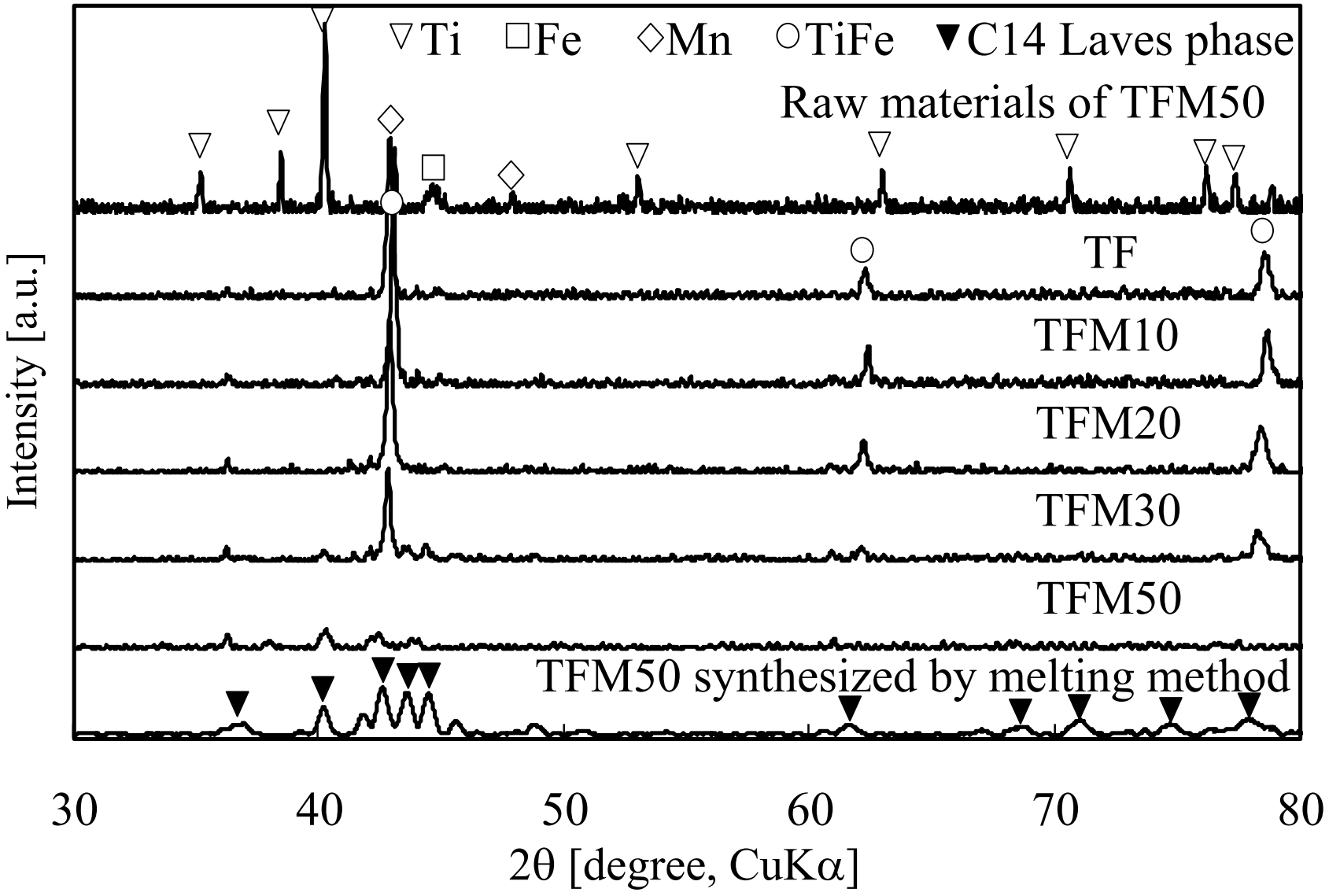

Fig. 3 XRD patterns of raw materials of TFM50 and SICSed $TiFe_{1-X}Mn_X$ (X=0 – 0.5) and melting method.

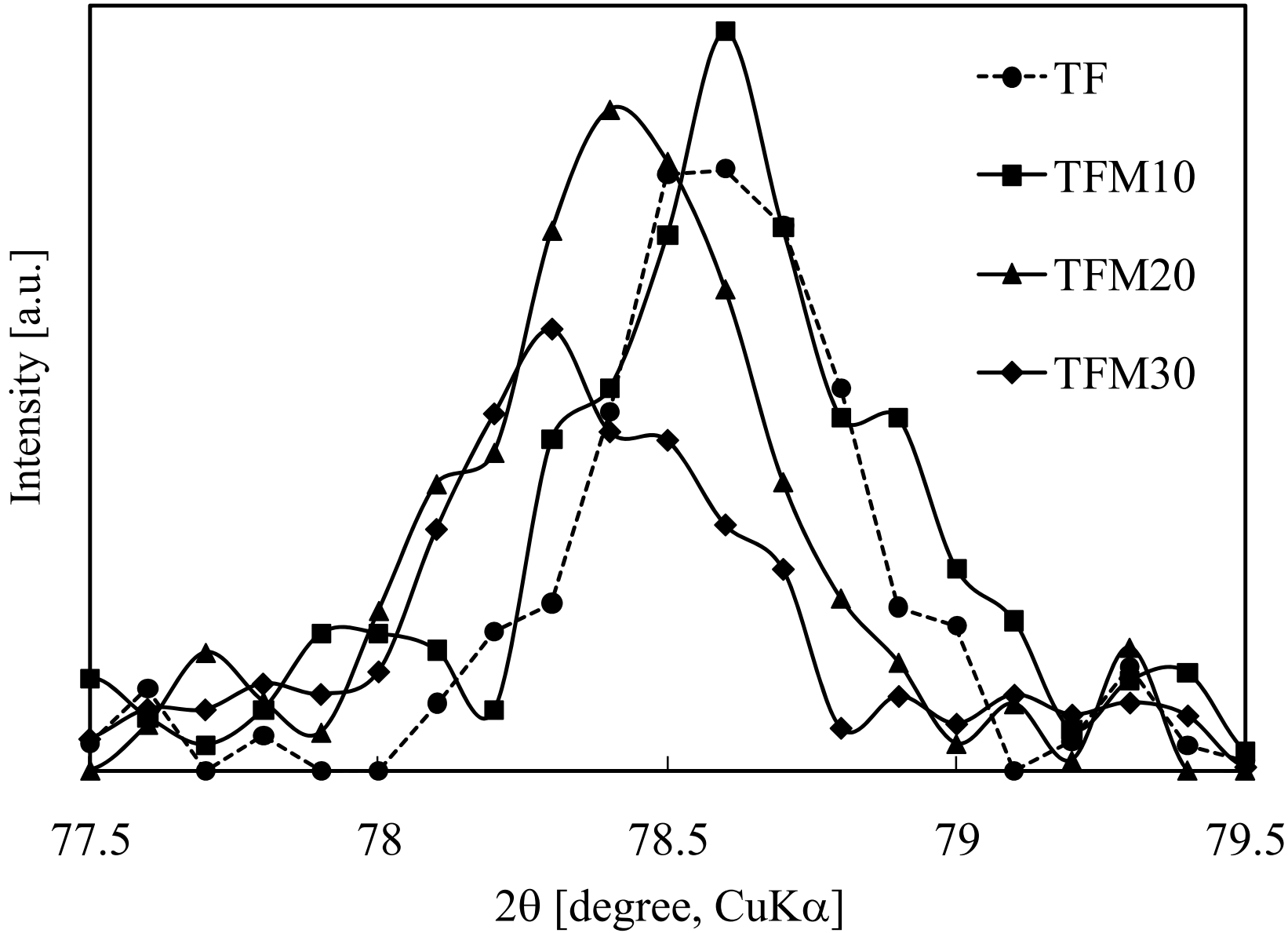

Fig. 4 Enlarged view of XRD patterns of SICSed $TiFe_{1-X}Mn_X$ (X=0 – 0.3).

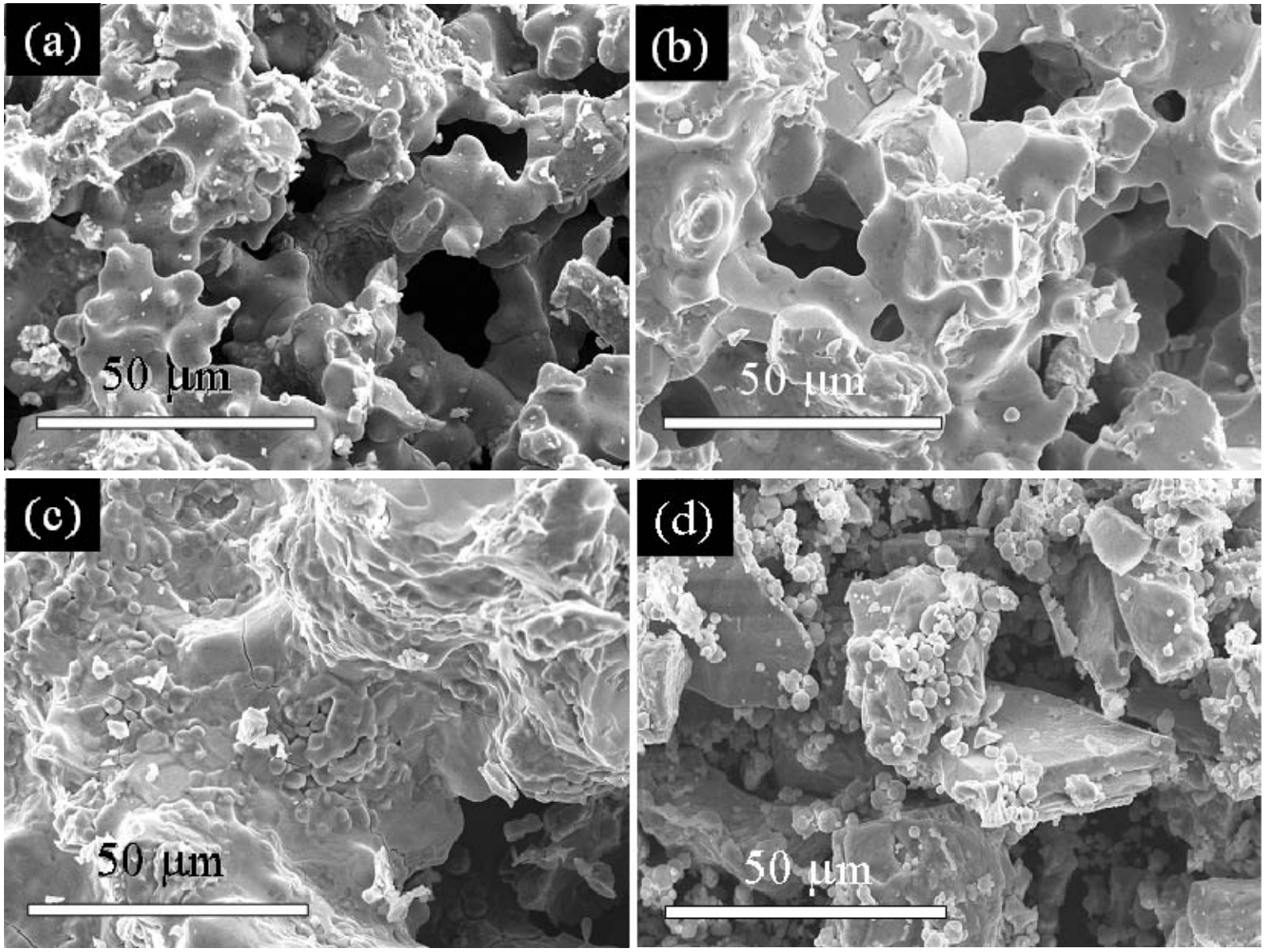

Fig. 5 SEM images of SICSed $TiFe_{1-X}Mn_X$ (X=0 – 0.5) and raw materials:
(a) TF; (b)TFM10; (c) TFM50; (d) Raw materials of TFM50.

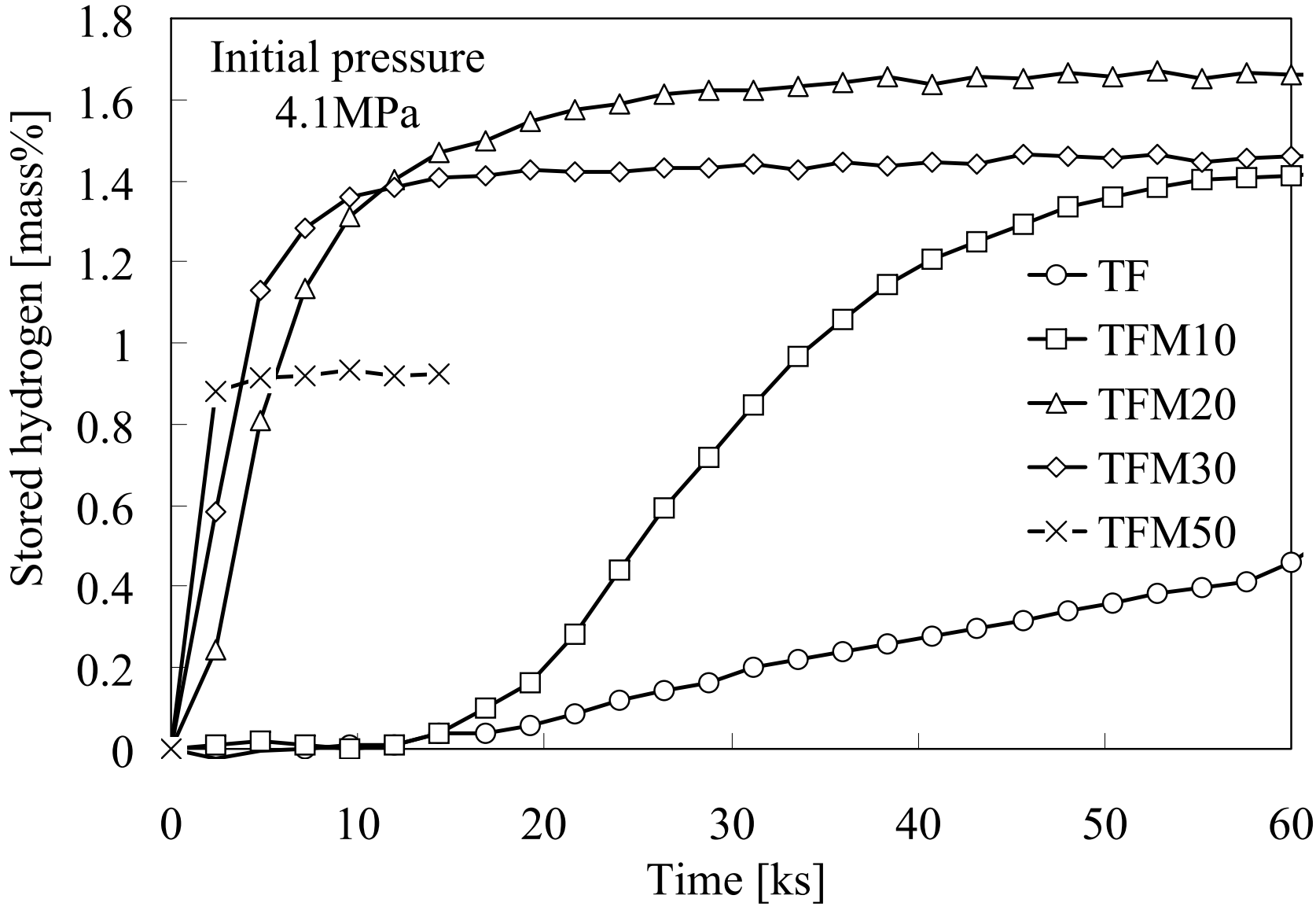

Fig. 6 Initial hydriding curves of SICSed $TiFe_{1-X}Mn_X$ (X=0 – 0.5) at 298K and under initial pressure of 4.1MPa.

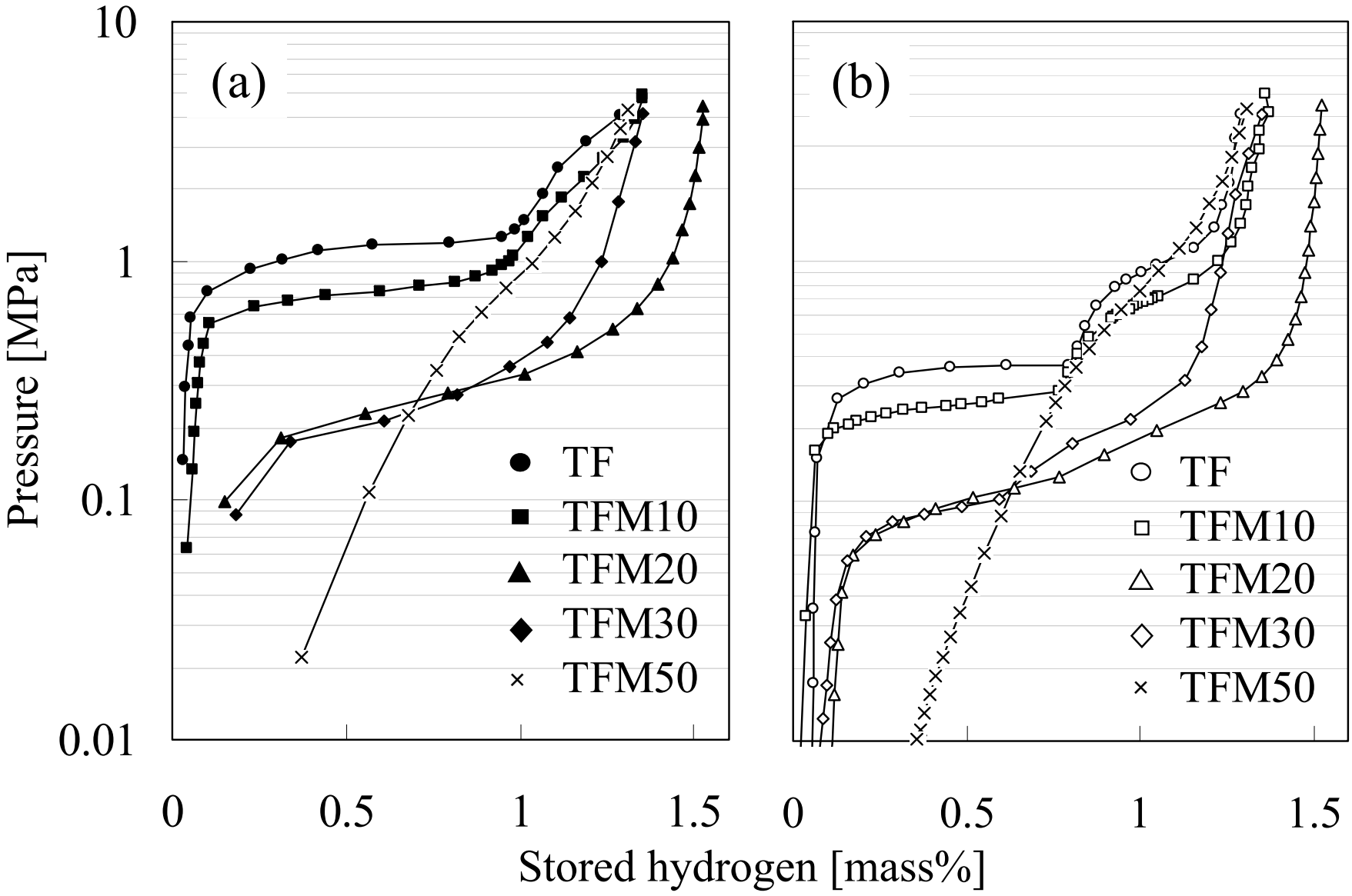

Fig. 7 PCT curves of SICSed $TiFe_{1-X}Mn_X$ (X=0 - 0.5) at 298K: (a) absorption; (b) desorption.

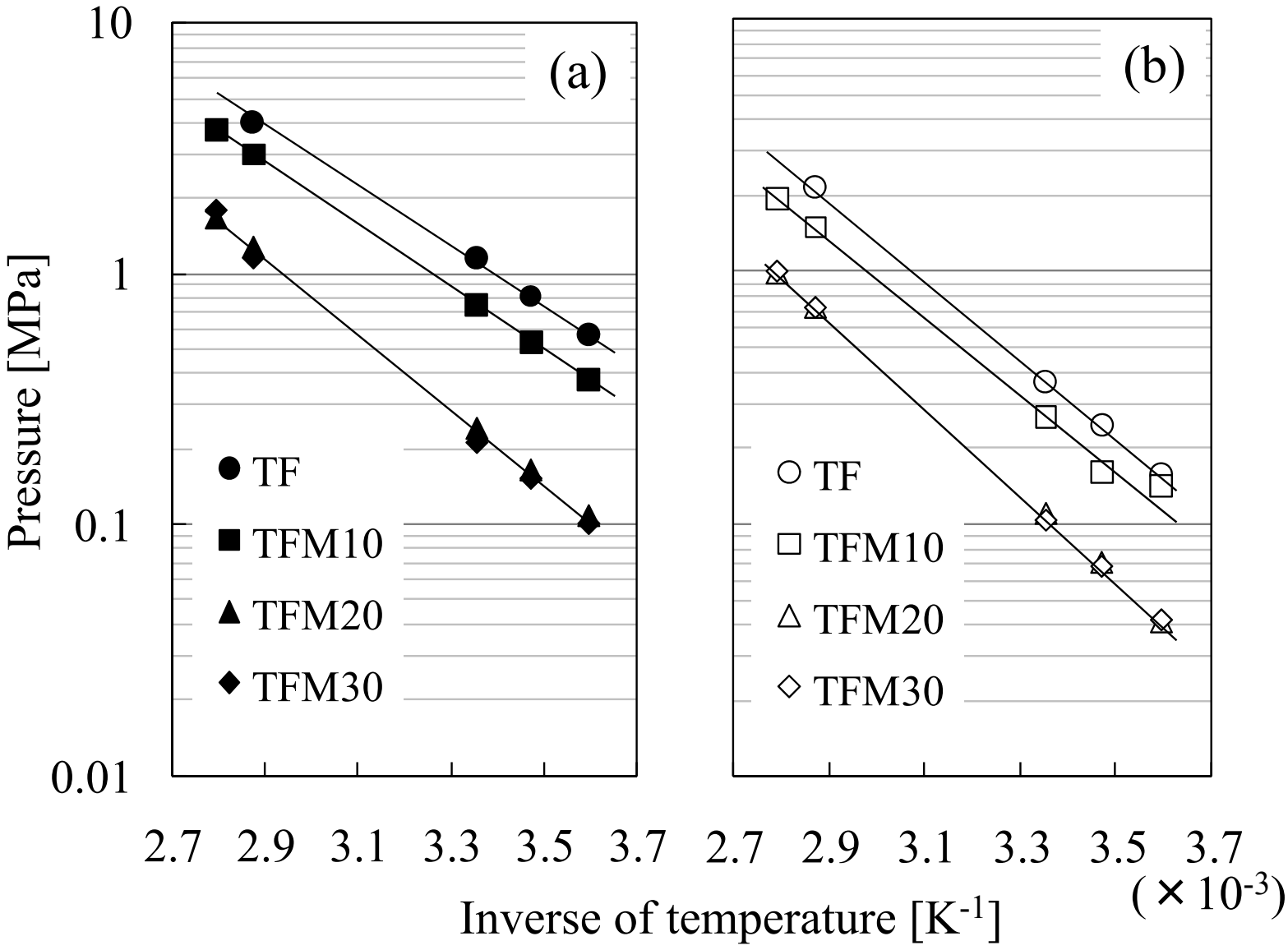

Fig. 8 Van't hoff plots for SICSed $TiFe_{1-X}Mn_X$ (X=0 - 0.3): (a) absorption; (b) desorption.